The Canadian Mineralogist
Vol. 52, pp. 77-89 (2014)
DOI: 10.3749/canmin.52.1.77

THE Ag–Pd–Se SYSTEM: PHASE RELATIONS INVOLVING MINERALS AND POTENTIAL NEW MINERALS

ANNA VYMAZALOVÁ§

Czech Geological Survey, Geologická 6, 152 00 Prague 5, Czech Republic

DMITRIY A. CHAREEV

Institute of Experimental Mineralogy RAS, Chernogolovka, Russia

ALEXANDR V. KRISTAVCHUK

Institute of Experimental Mineralogy RAS, Chernogolovka, Russia, and University of Dubna, Universitetskaja 19, Dubna, Russia

FRANTIŠEK LAUFEK AND MILAN DRÁBEK

Czech Geological Survey, Geologická 6, 152 00 Prague 5, Czech Republic

ABSTRACT

The phase equilibria in the system Ag–Pd–Se were studied by the evacuated-silica glass tube method at 350, 430, and 530 °C. In the system we synthesized four ternary phases: $Ag_2Pd_3Se_4$ (chrisstanleyite) and the new phases $AgPd_3Se$, $(Ag,Pd)_{22}Se_6$, and $Ag_6Pd_{74}Se_{20}$. The $AgPd_3Se$ phase forms a $Ag_{1-x}Pd_{3+x}Se$ (x = 0–0.15) solid-solution series. The $(Ag,Pd)_{22}Se_6$ phase forms a $(Ag_{11\pm x}Pd_{11\pm x})_{22}Se_6$ ($0.2 \geq x \geq 3.9$) solid-solution series, the solubility of Ag decreasing with increasing temperature. Palladseite ($Pd_{17}Se_{15}$) forms a limited solid solution and dissolves up to 7 wt.% Ag, and the phase Pd_9Se_2 dissolves up to 3 wt.% Ag. The $Ag_2Pd_3Se_4$ phase, an analogue of the mineral chrisstanleyite, forms stable associations with naumannite (Ag_2Se) and veerbekite ($PdSe_2$); it also coexists with palladseite (dissolving 7 wt.% Ag). The phase is stable up to 430 ºC. Phase relations determined the mineral assemblages that can be expected to occur in nature. Ternary $AgPd_3Se$ and $(Ag,Pd)_{22}Se_6$ phases and the binary PdSe, Pd_7Se_4, and $Pd_{34}Se_{11}$ phases can be expected in associations with the mineral palladseite, among other selenides. Finding these phases in nature is highly probable in telethermal selenide veins and unconformity-related uranium deposits, at conditions of high Se/S fugacity ratio, an oxidizing environment, and Se-rich fluids, forming at low temperatures. The $Ag_6Pd_{74}Se_{20}$ phase forms stable associations with $AgPd_3Se$ and Pd_7Se_2. It also coexists with Pd_4Se and Pd_9Se_2. The $Ag_6Pd_{74}Se_{20}$ phase is stable above 430 ºC. Under natural conditions the $Ag_6Pd_{74}Se_{20}$ and Pd_9Se_2 phases can be expected to occur in less traditional environments than are usual for selenides, forming at higher temperatures (above 430 ºC).

Keywords: Ag–Pd–Se system, phase relations, phase diagram, platinum-group minerals, chrisstanleyite, palladseite, Ag–Pd selenides

INTRODUCTION

In addition to the native elements Ag, Pd, and Se, the Ag–Pd–Se system comprises four minerals: palladseite ($Pd_{17}Se_{15}$), verbeekite (monoclinic $PdSe_2$), naumannite (Ag_2Se), and chrisstanleyite ($Ag_2Pd_3Se_4$). In nature, minerals belonging to the Ag–Pd–Se system occur in various geological environments. Palladium selenides are known to occur in auriferous mineralizations, also known as "jacutinga" type ores, in Minais Gerais and Serra Pelada in Brazil (Clark *et al.* 1974, Davis *et al.* 1977, Olivo & Gauthier 1995, Cabral *et al.* 2002, Cabral & Lehmann 2007) and have been observed in carbonaceous Precambrian black shales in the Voronezh crystalline massif in Russia (Rudashevskiy *et al.* 1995). Chrisstanleyite was found in gold-bearing carbonate veins in Middle Devonian limestones at Hope's Nose, Torquay, Devon in England (Paar *et al.* 1998), and

§ *Corresponding author e-mail address*: anna.vymazalova@geology.cz

has also been reported from the Musonoi Cu-Co-Mn-U mine of the Shaba province in the Democratic Republic of Congo (Roberts *et al.* 2002), Tilkerode in the eastern Harz Mountains in Germany (Stanley *et al.* 2002), in selenide mineralization at El Chire in Argentina (Paar *et al.* 2004), in uranium mineralization at Předbořice, Czech Republic (Paar *et al.* 2005), the East Pilbara region of Western Australia (Nickel 2002), and from Gongo Soco in Minas Gerais, Brazil (Cabral & Lehmann 2007). Verbeekite is known from its type locality, the Musonoi Cu-Co-Mn-U mine in the Democratic Republic of Congo (Roberts *et al.* 2002) and Hope's Nose in Devon in England (Paar *et al.* 1998).

Selenides are closely associated with sulfides, oxides, tellurides, and native elements in a variety of mineral assemblages; Se, being strongly chalcophile, often substitutes for S in sulfides. Simon *et al.* (1997) reviewed the mineralogy of selenides in natural ore deposits using the thermodynamic data and calculated equilibria for binary selenides presented by Simon & Essene (1996).

Selenides are formed from hydrothermal fluids at conditions of high Se/S fugacity ratio. According to the study of Simon *et al.* (1997), an oxidizing environment (close to the anglesite-galena buffer) and Se-rich fluids are essential to form most selenide minerals. Selenium-rich, relatively reduced (below the hematite-magnetite buffer) hydrothermal fluids can deposit only Ag selenides; no other selenide minerals can deposit from such fluids. Selenides are found in four main types of deposits: telethermal selenide veins, unconformity-related uranium deposits, sandstone-hosted uranium deposits, and epithermal Au-Ag deposits (Simon *et al.* 1997). Telethermal selenide vein-type deposits include the well-known selenide-bearing deposits in the Harz Mountains in Germany (Clausthal, Lerbach, Tilkerode, Trogtal, and Zorge; Tischendorf 1959, Wallis 1994, Stanley *at al.* 2002), and in Bolivia (El Dragón, Grundmann *et al.* 1990; Pacajake, *e.g.*, Ahlfeld 1941) and Argentina (La Rioja province, *e.g.*, Paar *et al.* 1996), or the selenide occurrences at Hope's Nose in Devon, England (Stanley *et al.* 1990). Unconformity-related U deposits contain selenide-bearing mineralization in the Bohemian Massif (Předbořice, Petrovice, Habry; Kvaček 1979, Johan 1989), in the Massif Central in France (*e.g.*, Johan *et al.* 1982), and in the Athabasca area of Saskatchewan (*e.g.*, Robinson 1955). Palladium selenides are known to occur predominatly in telethermal selenide veins and unconformity-related U deposits; in these deposits they formed at low temperatures, below 300 °C (Simon *et al.* 1997).

In this contribution we present phase relations in the Ag–Pd–Se system in three isothermal sections.

Previous Experiments

The binary Pd–Se system

The binary system Pd–Se was revised and evaluated by Okamoto (1992) based on the data of Olsen *et al.* (1979) and Takabatake *et al.* (1987); the binary diagram is shown in Figure 1. The system comprises eight inter-

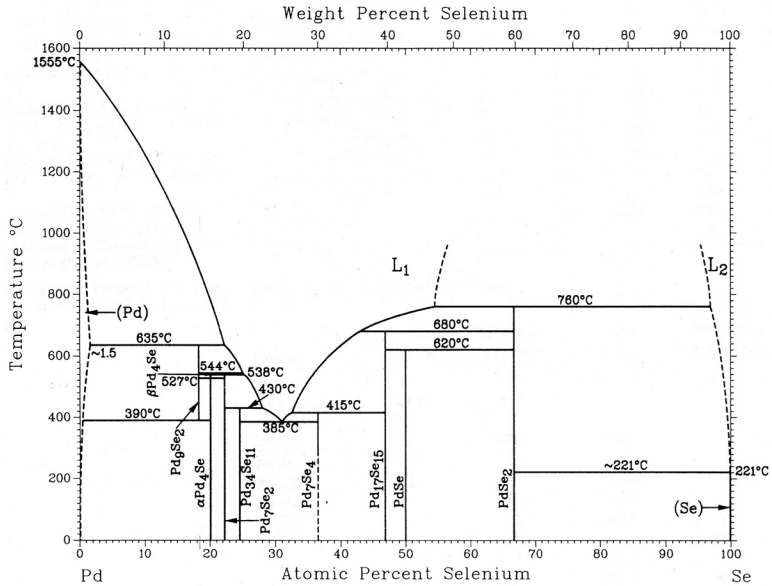

FIG. 1. Phase diagram of the binary system Pd–Se, taken from Okamoto (1992), primarily based on data from Olsen *et al.* (1979) and Takabatake *et al.* (1987).

mediate phases: Pd_4Se, Pd_9Se_2 (stable in the temperature interval from 390 to 635 °C), Pd_7Se_2, $Pd_{34}Se_{11}$, Pd_7Se_4, $Pd_{17}Se_{15}$, PdSe, and $PdSe_2$.

The binary Ag–Pd and Ag–Se systems

Karakaya & Thompson (1988) reported complete (Ag, Pd) solid solution. In the Ag–Se system only two Ag_2Se phases exist with two polymorphic modifications (α and β) (Karakaya & Thompson 1990, Hansen & Anderko 1958).

The ternary Ag–Pd–Se system

Phase relations in the ternary Ag–Pd–Se system have not been studied to date. Paar *et al*. (1998) described the ternary mineral chrisstanleyite ($Ag_2Pd_3Se_4$), and Laufek *et al*. (2011, 2013) published a preliminary report concerning the crystal structures of the $AgPd_3Se$ and $(Ag,Pd)_{22}Se_6$ phases.

The structural data for phases and minerals in the Ag–Pd–Se system are summarized in Tables 1 and 2, respectively.

Methods and Techniques

Experimental

Experiments were performed in evacuated and sealed silica glass tubes in horizontal tube furnaces, following the method of Kullerud (1971). To prevent loss of material to the vapor phase during experiments, the free space in the tubes was reduced by placing close-fitting glass rods over the charge. The temperatures were measured with Pt-PtRh thermocouples and are accurate to within ± 3 °C. Charges of 100 to 200 mg were carefully weighed out from the native elements. We used silver powder (Aldrich Chem. Co., 99.999% purity), Se pebbles (Aldrich Chem. Co., 99.999% purity), and Pd powder (Aldrich Chem. Co., 99.95% purity) as starting materials. The starting mixtures were first melted at 1200 °C for three days. Then the products from the 1200 °C melting were ground in an agate mortar under acetone and reheated to 350 °C (for 120 days), 430 °C (90 days), and 530 °C (70 days). In order to attain equilibrium, the experimental products were reground under acetone and reheated to the required temperature. After heating, quenching was done by dropping the capsules in cold water. A list of representative experimental starting materials and products is given in Table 3 and plotted in Figure 2. Phases in the experimental products were characterized by X-ray powder diffraction, in polished sections examined in reflected light, and with electron-microprobe techniques. In a few experiments exsolution was observed that was caused by the sluggish quench from 430 or 530 °C. When the experiment was repeated and rapidly quenched the exsolution was no longer observed.

X-ray diffraction analysis

Each experimental product was primarily studied with powder X-ray diffraction (XRD). Powder X-ray diffraction data for the products were collected with

TABLE 1. CRYSTALLOGRAPHIC DATA FOR SYNTHETIC PHASES IN THE SYSTEM Ag–Pd–Se

Phase	Crystal Structure		Unit cell parameters				Reference
			a (Å)	*b* (Å)	*c* (Å)	β (°)	
βAg_2Se	cubic	$Im\bar{3}m$	4.983				1
αAg_2Se	orthorhombic	$P2_12_12$	4.333	7.062	7.764		2
Pd_9Se_2	trigonal						3
βPd_4Se	unknown						
αPd_4Se	tetragonal	$P\bar{4}2_1c$	5.2302		5.6461		4*
Pd_7Se_2	monoclinic	$P2_1/a$	9.4539	5.3520	5.4967	93.509	5*
$Pd_{34}Se_{11}$	monoclinic	$P2_1/n$	21.454	5.5052	12.0348	99.454	5*
Pd_7Se_4	orthorombic	$P2_122_1$	6.8618	5.3793	10.1613		6*
$Pd_{17}Se_{15}$	cubic	$Pm\bar{3}m$		10.6048			7*
PdSe	tetragonal	$P4_2/m$	6.7248		6.9128		8*
$PdSe_2$	orthorombic	$Pbca$	5.7394	5.8624	7.6926		9*
$Ag_2Pd_3Se_4$	monoclinic	$P2_1/c$	5.6872(2)	10.410(1)	6.3545(3)	114.91(1)	this study
$AgPd_3Se$	cubic	$Pa\bar{3}$	8.6289				10
$(Ag,Pd)_{22}Se_6$	cubic	$Fm\bar{3}m$	12.3169				11

Notes: Crystal structure data are from: [1]Rahlfs (1936), [2]Wiegers (1971), [3]Takabatake *et al*. (1987), [4]Grønvold & Røst (1962), [5]Sato *et al*. (1989), [6]Matkovic & Schubert (1978), [7]Geller (1962), [8]Ijjaali & Ibers (2001), [9]Grønvold & Røst (1957), [10]Laufek *et al*. (2011), [11]Laufek *et al*. (2013)
*Unit cell data are taken from Vymazalová *et al*. (2011).

TABLE 2. CRYSTALLOGRAPHIC DATA FOR MINERALS IN THE Ag–Pd–Se SYSTEM

Mineral		Crystal Structure		Unit cell parameters				Reference
				a (Å)	*b* (Å)	*c* (Å)	β (°)	
naumannite	Ag_2Se	orthorombic	$P2_12_12$	4.333	7.062	7.764		1
palladseite	$Pd_{17}Se_{15}$	cubic	$Pm\bar{3}m$		10.635			2
verbeekite	$PdSe_2$	monoclinic	*C*2/*m*, *C*2 or *Cm*	6.659	4.124	4.438	92.76	3
chrisstanleyite	$Ag_2Pd_3Se_4$	monoclinic	$P2_1/c$	6.676	10.342	6.341	114.996	4

Notes: [1]Wiegers (1971), [2]Davis *et al.* (1977), [3]Roberts *et al.* (2002), [4]Topa *et al.* (2006).

TABLE 3. RESULTS OF SELECTED EXPERIMENTS IN THE Ag–Pd–Se SYSTEM

Experiment No.	Starting composition	Temperature/°C	Phase assemblages
A9	$Ag_{22.2}Pd_{33.3}Se_{44.4}$	350	$Ag_2Pd_3Se_4$
		430	Ag_2Se, $Pd_{17}Se_{15}$, $PdSe_2$
		530	Ag_2Se, $Pd_{17}Se_{15}$, $PdSe_2$
A10	$Ag_{40}Pd_{40}Se_{20}$	350	$(Ag,Pd)_{22}Se_6$
		430	$(Ag,Pd)_{22}Se_6$, Ag-Pd
		530	$(Ag,Pd)_{22}Se_6$, Ag-Pd
A11	$Ag_{20}Pd_{55}Se_{25}$	350	$(Ag,Pd)_{22}Se_6$, $AgPd_3Se$, $Pd_{17}Se_{15}$
		430	$(Ag,Pd)_{22}Se_6$, $AgPd_3Se$, $Pd_{17}Se_{15}$
		530	$AgPd_3Se$, Ag_2Pd_2Se, *L* (Pd,Se)
A12	$Ag_{20}Pd_{30}Se_{50}$	350	$Ag_2Pd_3Se_4$, Ag_2Se, $PdSe_2$
		430	Ag_2Se, $Pd_{17}Se_{15}$, $PdSe_2$
		530	Ag_2Se, $Pd_{17}Se_{15}$, $PdSe_2$
A13	$Ag_{30}Pd_{40}Se_{30}$	350	$(Ag,Pd)_{22}Se_6$, $Pd_{17}Se_{15}$
		430	$(Ag,Pd)_{22}Se_6$, $Pd_{17}Se_{15}$
		530	$(Ag,Pd)_{22}Se_6$, $Pd_{17}Se_{15}$
A14	$Ag_{33.3}Pd_{25}Se_{41.7}$	350	$Ag_2Pd_3Se_4$, Ag_2Se
		430	Ag_2Se, $Pd_{17}Se_{15}$, $PdSe_2$
		530	Ag_2Se, $Pd_{17}Se_{15}$, $PdSe_2$
A15	$Ag_{20}Pd_{40}Se_{40}$	350	$(Ag,Pd)_{22}Se_6$, $Pd_{17}Se_{15}$, Ag_2Se
		430	$(Ag,Pd)_{22}Se_6$, $Pd_{17}Se_{15}$, Ag_2Se
		530	$(Ag,Pd)_{22}Se_6$, $Pd_{17}Se_{15}$, Ag_2Se
A16	$Ag_{20}Pd_{20}Se_{60}$	350	Se, Ag_2Se, $PdSe_2$
		430	Se_l, Ag_2Se, $PdSe_2$
		530	Se_l, Ag_2Se, $PdSe_2$
A17	$Ag_6Pd_{47}Se_{47}$	350	$Pd_{17}Se_{15}$, $PdSe_2$
		430	$Pd_{17}Se_{15}$, $PdSe_2$
		530	$Pd_{17}Se_{15}$, $PdSe_2$
A18	$Ag_{22.5}Pd_{34}Se_{43.5}$	350	$Ag_2Pd_3Se_4$, Ag_2Se, $Pd_{17}Se_{15}$
		430	Ag_2Se, $Pd_{17}Se_{15}$, $PdSe_2$
		530	Ag_2Se, $Pd_{17}Se_{15}$, $PdSe_2$
A19	$Ag_{20}Pd_{60}Se_{20}$	350	$AgPd_3Se$
		430	$AgPd_3Se$
		530	$AgPd_3Se$
A20	$Ag_{60}Pd_{20}Se_{20}$	350	$(Ag,Pd)_{22}Se_6$, Ag_2Se, Ag-Pd
		430	$(Ag,Pd)_{22}Se_6$, Ag_2Se, Ag-Pd
		530	$(Ag,Pd)_{22}Se_6$, Ag_2Se, Ag-Pd
A21	$Ag_{30}Pd_{50}Se_{20}$	350	$(Ag,Pd)_{22}Se_6$, $AgPd_3Se$
		430	$(Ag,Pd)_{22}Se_6$, $AgPd_3Se$
		530	$(Ag,Pd)_{22}Se_6$, $AgPd_3Se$
A22	$Ag_{20}Pd_{50}Se_{30}$	350	$(Ag,Pd)_{22}Se_6$, $AgPd_3Se$, $Pd_{17}Se_{15}$
		430	$(Ag,Pd)_{22}Se_6$, $AgPd_3Se$, $Pd_{17}Se_{15}$
		530	$(Ag,Pd)_{22}Se_6$, $Pd_{17}Se_{15}$, *L*

Heating time: 120 at days 350 °C, 90 days at 430 °C, 70 days at 530 °C

TABLE 3. – continued

Experiment No.	Starting composition	Temperature/°C	Phase assemblages
A23	$Ag_{10}Pd_{60}Se_{30}$	350	$AgPd_3Se$, $Pd_{17}Se_{15}$, $Pd_{34}Se_{11}$
		430	$AgPd_3Se$, $Pd_{17}Se_{15}$, *L*
		530	$AgPd_3Se$, $Pd_{17}Se_{15}$, *L*
A24	$Ag_{25}Pd_{45}Se_{30}$	350	$(Ag,Pd)_{22}Se_6$, $Pd_{17}Se_{15}$
		430	$(Ag,Pd)_{22}Se_6$, $Pd_{17}Se_{15}$
		530	$(Ag,Pd)_{22}Se_6$, $Pd_{17}Se_{15}$
A25	$Ag_7Pd_{70}Se_{23}$	350	$AgPd_3Se$, $Pd_{34}Se_{11}$
		430	$AgPd_3Se$, Pd_7Se_2, *L*
		530	$AgPd_3Se$, Pd_7Se_2, *L*
A26	$Ag_{15}Pd_{70}Se_{15}$	350	$AgPd_3Se$, Pd_4Se, Ag-Pd
		430	$AgPd_3Se$, $Ag_6Pd_{74}Se_{20}$, Ag-Pd
		530	$AgPd_3Se$, $Ag_6Pd_{74}Se_{20}$, Ag-Pd
A27	$Ag_{40}Pd_{45}Se_{15}$	350	$(Ag,Pd)_{22}Se_6$, $AgPd_3Se$, Ag-Pd
		430	$(Ag,Pd)_{22}Se_6$, $AgPd_3Se$, Ag-Pd
		530	$(Ag,Pd)_{22}Se_6$, $AgPd_3Se$, Ag-Pd
A28	$Ag_7Pd_{73}Se_{20}$	350	$AgPd_3Se$, Pd_7Se_2
		430	$AgPd_3Se$, Pd_7Se_2
		530	$AgPd_3Se$, Pd_7Se_2
A29	$Ag_2Pd_{45}Se_{53}$	350	$PdSe_2$, $Pd_{17}Se_{15}$
		430	$PdSe_2$, $Pd_{17}Se_{15}$
		530	$PdSe_2$, $Pd_{17}Se_{15}$
A30	$Ag_{55}Pd_{30}Se_{15}$	350	$(Ag,Pd)_{22}Se_6$, Ag-Pd
		430	$(Ag,Pd)_{22}Se_6$, Ag-Pd
		530	$(Ag,Pd)_{22}Se_6$, Ag-Pd
A31	$Ag_2Pd_{56}Se_{42}$	350	$Pd_{17}Se_{15}$, Pd_7Se_4
		430	$Pd_{17}Se_{15}$, *L*
		530	$Pd_{17}Se_{15}$, *L*
A32	$Ag_{33}Pd_{46}Se_{21}$	350	$(Ag,Pd)_{22}Se_6$, $AgPd_3Se$
		430	$(Ag,Pd)_{22}Se_6$, $AgPd_3Se$
		530	$(Ag,Pd)_{22}Se_6$, $AgPd_3Se$
A33	$Ag_1Pd_{51}Se_{48}$	350	$Pd_{17}Se_{15}$, PdSe
		430	$Pd_{17}Se_{15}$, PdSe
		530	$Pd_{17}Se_{15}$, PdSe
A34	$Ag_6Pd_{73}Se_{21}$	350	$AgPd_3Se$, Pd_4Se, traces Ag-Pd
		430	$Ag_6Pd_{74}Se_{20}$, traces Pd_9Se_2
		530	$Ag_6Pd_{74}Se_{20}$, traces Pd_9Se_2
A35	$Ag_{33}Pd_{33}Se_{33}$	350	$(Ag,Pd)_{22}Se_6$, $Pd_{17}Se_{15}$, Ag_2Se
		430	$(Ag,Pd)_{22}Se_6$, $Pd_{17}Se_{15}$, Ag_2Se
		530	$(Ag,Pd)_{22}Se_6$, $Pd_{17}Se_{15}$, Ag_2Se
A36	$Ag_{50}Pd_{20}Se_{30}$	350	$(Ag,Pd)_{22}Se_6$, $Pd_{17}Se_{15}$, Ag_2Se
		430	$(Ag,Pd)_{22}Se_6$, $Pd_{17}Se_{15}$, Ag_2Se
		530	$(Ag,Pd)_{22}Se_6$, $Pd_{17}Se_{15}$, Ag_2Se

Heating time: 120 at days 350 °C, 90 days at 430 °C, 70 days at 530 °C

a Philips X´Pert diffractometer using Cu*K*α radiation. The data were collected in the 2θ theta range from 10 to 140°, with a step of 0.02°. The whole-profile-fitting method (WPPF) was applied to calculate unit-cell parameters from powder data, using the FULLPROF program (Rodríguez-Carvajal 2006).

Electron-microprobe analyses

Chemical analyses were performed with a CAMECA SX-100 electron probe microanalyzer (EPMA) in wavelength-dispersion mode using an electron beam focused to 1–2 μm. Pure elements were used as standards. Concentrations were quantified on the PdLα, AgLβ, and SeLα lines with an accelerating voltage of 15 keV and a beam current of 10 nA on the Faraday cup. In each sample, compositional data were collected from several grains within a polished section (minimum n = 5) and then averaged. Electron probe microanalysis data are presented in Table 4.

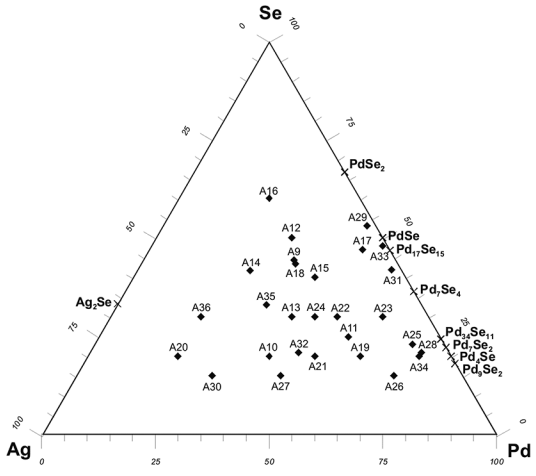

FIG. 2. Experimental starting compositions in the ternary phase diagram.

RESULTS AND DISCUSSION

Phase relations

The Ag–Pd–Se system was studied at 350, 430, and 530 °C. Phase assemblages based on EPMA and powder XRD data are listed in Table 3; phase compositions are given in Table 4. The starting compositions are plotted in Figure 2. Three isothermal sections at 350, 430, and 530 °C are presented in Figure 3.

Phase relations at 350 °C

The isothermal section for 350 °C is shown in Figure 3a. At 350 °C, the system contains three ternary compounds: $Ag_2Pd_3Se_4$, $(Ag,Pd)_{22}Se_6$, and $AgPd_3Se$. Stable assemblages are listed in Table 5. The phase $Pd_{17}Se_{15}$, the analogue of palladseite, dissolves up to 7 wt.% Ag; the range of solid solution does not change with increasing temperature. The solid solution of

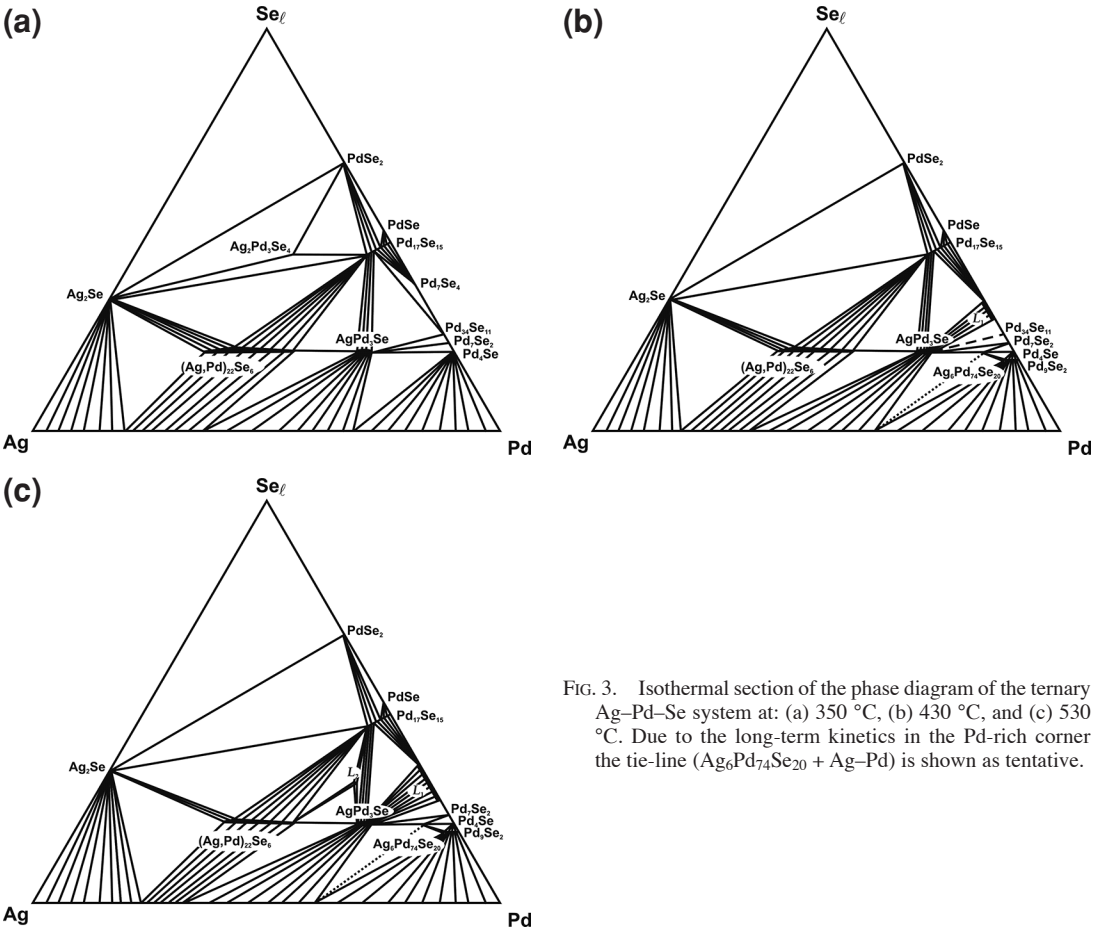

FIG. 3. Isothermal section of the phase diagram of the ternary Ag–Pd–Se system at: (a) 350 °C, (b) 430 °C, and (c) 530 °C. Due to the long-term kinetics in the Pd-rich corner the tie-line ($Ag_6Pd_{74}Se_{20}$ + Ag–Pd) is shown as tentative.

$Ag_{1-x}Pd_{3+x}Se_{ss}$ extends from $Ag_{0.86}Pd_{3.16}Se_{0.98}$ up to composition $Ag_{1.01}Pd_{3.00}Se_{0.99}$ and remains constant with increasing temperature. The $(Ag_{11\pm x}Pd_{11\pm x})_{\sum 22}Se_6$ solid solution extends from $(Ag_{8.99}Pd_{13.13})_{\sum 22.12}Se_{5.88}$ (34.2 wt.% Ag) to $(Ag_{14.83}Pd_{7.32})_{\sum 22.16}Se_{5.85}$ (55.9 wt.% Ag) at 350 °C; the solubility of Ag decreases with increasing temperature (Fig. 4).

Phase relations define the mineral assemblages that can be expected to occur in nature. Binary and ternary phases which are unknown as minerals coexist with phases that do occur naturally. For example, Pd_7Se_4 and $Pd_{34}Se_{11}$, unknown as minerals, coexist with palladseite, and $(Ag,Pd)_{22}Se_6$ coexists with naumannite and palladseite. Ternary phases $AgPd_3Se$ and $(Ag,Pd)_{22}Se_6$ and the binary phases PdSe, Pd_7Se_4, and $Pd_{34}Se_{11}$ can be expected in associations with the mineral palladseite, among other selenides. Finding these phases is highly probable in telethermal selenide veins and unconformity-related uranium types of deposits.

Phase relations at 430 °C

The isothermal section for 430 °C is shown in Figure 3b. Phase relations are similar to those for 350 °C; however, at this temperature phases $Ag_2Pd_3Se_4$ (stability limit: 430 °C), Pd_7Se_4 (stability limit: 415 °C, Olsen *et al.* 1979), and $Pd_{34}Se_{11}$ (stability limit: 430 °C, Takabatake *et al.* 1987) are no longer stable. On the contrary, phases $Ag_6Pd_{74}Se_{20}$ and Pd_9Se_2 become stable. At 385 °C (Okamoto 1992) a binary eutectic liquid between $Pd_{34}Se_{11}$ and Pd_7Se_4 appears in the system. Subsequently assemblages $Ag_2Se + PdSe_2 + Ag_2Pd_3Se_4$; $Ag_2Pd_3Se_4 + PdSe_2 + Pd_{17}Se_{15\ ss}$; $Ag_2Se + Ag_2Pd_3Se_4 + Pd_{17}Se_{15\ ss}$; $Pd_{17}Se_{15\ ss} + Pd_7Se_4 + Pd_{34}Se_{11}$; and $Ag_{1-x}Pd_{3+x}Se_{ss} + Pd_{34}Se_{11} + Pd_7Se_2$ disappear from the system and new assemblages appear in the system (Table 5). At 430 °C, the solid solution $(Ag_{11\pm x}Pd_{11\pm x})_{\sum 22}Se_6$ slightly decreases compared to at 350 °C (Fig. 4); the range extends from $(Ag_{8.99}Pd_{13.11})_{\sum 22.11}Se_{5.89}$ (33.9 wt.% Ag) to $(Ag_{13.29}Pd_{8.93})_{\sum 22.22}Se_{5.78}$ (50.0 wt.% Ag).

TABLE 4. COMPOSITIONAL DATA FOR THE STUDIED PHASES

wt.%	Ag				Pd				Se					*apfu*			
No.		Min	Max	Std.dev.		Min	Max	Std.dev.		Min	Max	Std.dev.	Total	Ag	Pd	Se	∑(Ag,Pd)
								$Ag_2Pd_3Se_4$									
A9	25.46	25.05	25.86	0.34	37.94	37.31	38.57	0.54	36.40	36.05	36.41	0.17	99.79	2.02	3.05	3.94	
A12	25.39	25.36	25.42	0.02	37.94	37.54	38.17	0.28	35.82	35.72	35.95	0.09	99.15	2.03	3.07	3.90	
A14	24.66	23.91	25.15	0.54	37.89	37.75	38.07	0.14	36.11	35.76	36.69	0.42	98.65	1.97	3.08	3.95	
A18	23.77	23.21	24.21	0.42	38.03	37.59	38.72	0.49	37.07	37.05	37.11	0.02	98.87	1.89	3.07	4.03	
								$(Ag,Pd)_{22}Se_6$									
A10	40.89	40.45	41.67	0.45	42.42	41.83	42.84	0.37	16.01	15.85	16.16	0.11	99.32	10.82	11.39	5.79	22.21
A13	47.64	46.58	48.50	0.33	35.16	34.76	35.40	0.28	16.47	16.20	16.99	0.37	99.27	12.61	9.43	5.96	22.04
A15	48.41	48.22	49.59	0.38	33.84	33.22	34.45	0.45	16.63	16.00	17.22	0.44	98.88	12.86	9.11	6.03	21.97
A20	55.89	56.07	56.30	0.11	27.30	27.08	27.67	0.30	16.05	16.18	16.23	0.03	99.77	14.83	7.32	5.85	22.16
A21	35.12	34.75	35.49	0.31	47.89	47.42	48.08	0.20	16.37	16.34	16.39	0.03	99.38	9.28	12.82	5.90	22.10
A22	34.22	33.94	34.50	0.28	49.38	49.36	49.40	0.02	16.43	16.37	16.48	0.05	100.03	8.99	13.13	5.88	22.12
A24	39.26	38.62	39.90	0.64	44.44	44.29	44.58	0.15	16.64	16.26	17.01	0.38	100.33	10.13	11.87	6.01	21.99
A27	35.65	35.61	35.70	0.05	47.45	47.04	47.86	0.41	16.24	16.24	16.25	0.00	99.35	9.42	12.71	5.86	22.14
A30	49.04	48.64	49.23	0.29	33.29	32.79	33.69	0.37	16.13	16.05	16.22	0.07	98.47	13.10	9.01	5.89	22.11
A32	36.47	35.63	36.77	0.34	47.38	45.31	46.51	0.09	16.00	15.97	16.02	0.02	99.85	9.67	12.49	5.85	22.15
A35	47.42	47.20	47.64	0.22	35.59	35.39	35.80	0.21	16.62	16.43	16.82	0.19	99.64	12.50	9.51	5.99	22.01
A36	48.08	47.71	48.75	0.48	35.30	34.98	35.65	0.27	16.52	16.45	16.62	0.07	99.90	12.65	9.41	5.94	22.06
								$AgPd_3Se$									
A11	21.46	21.35	21.55	0.08	62.98	62.47	63.20	0.30	15.36	15.23	15.63	0.16	99.80	1.01	3.00	0.99	
A19	21.14	21.00	24.27	0.12	63.85	63.33	64.04	0.31	15.02	14.88	15.13	0.10	100.00	0.99	3.04	0.96	
A21	21.42	21.35	21.55	0.09	62.73	62.47	63.16	0.30	15.39	15.33	15.63	0.18	99.54	1.01	3.00	0.99	
A22	21.35	21.43	21.52	0.04	62.53	63.07	63.20	0.07	15.36	15.23	15.26	0.01	99.86	1.01	3.01	0.98	
A23	18.91	18.72	19.09	0.15	65.42	65.07	65.81	0.30	15.50	15.45	15.59	0.06	99.83	0.89	3.12	1.00	
A25	18.82	18.37	19.05	0.32	65.93	65.65	66.13	0.20	15.24	15.14	15.34	0.08	99.99	0.88	3.14	0.98	
A26	18.36	18.18	18.53	0.17	66.28	66.19	66.37	0.09	15.19	15.17	15.21	0.02	99.82	0.86	3.16	0.98	
A27	21.64	21.35	21.92	0.29	63.13	63.11	63.16	0.03	15.28	15.23	15.33	0.05	100.05	1.02	3.00	0.98	
A28	18.35	18.18	15.52	0.17	65.72	66.16	65.28	0.44	15.16	15.15	15.17	0.01	99.23	0.87	3.15	0.98	
A32	21.44	21.35	21.53	0.09	62.98	61.80	63.16	0.18	15.24	15.15	15.33	0.09	99.72	1.02	3.00	0.99	
A34	18.47	18.37	18.53	0.07	66.06	65.65	66.37	0.30	15.20	15.15	15.25	0.04	99.73	0.87	3.15	0.98	

d.l.: below detection limit

TABLE 4. – continued

wt.%	Ag				Pd				Se					*apfu*		
No.		Min	Max	Std.dev.		Min	Max	Std.dev.		Min	Max	Std.dev.	Total	Ag	Pd	Se
								$Ag_6Pd_{74}Se_{20}$								
A34*	6.70	6.44	6.91	0.14	77.85	77.28	78.47	0.36	15.25	15.21	15.34	0.04	99.80	6.29	74.14	19.57
								Ag_2Se								
A12	73.33	72.95	73.52	0.27	0.16	0.10	0.28	0.08	26.08	26.01	26.23	0.10	99.58	2.02		0.98
A14	73.27	73.01	73.53	0.26	d.l.				25.85	25.51	26.19	0.34	99.23	2.01		0.99
A16	73.14	72.94	73.52	0.27	0.22	0.10	0.28	0.08	26.15	26.01	26.24	0.10	99.52	2.01	0.01	0.98
A20	72.84	72.97	72.99	0.01	d.l.				26.46	26.48	26.49	0.01	99.45	2.01		0.99
A35	74.17	72.97	74.87	0.70	d.l.				26.11	25.75	26.48	0.36	100.31	2.02		0.98
A36	72.54	72.97	73.02	0.02	0.10				26.41	26.48	26.51	0.02	99.49	2.00		1.00
								Ag–Pd								
A20	79.95	79.49	80.40	0.46	19.48	19.43	19.53	0.05	0.65	0.62	0.68	0.03	100.08	0.79	0.20	0.01
A26	30.59	30.40	30.77	0.15	67.91	67.40	68.29	0.38	1.01	1.00	1.02	0.01	99.52	0.30	0.68	0.01
A27	63.68	63.67	63.70	0.01	35.82	35.47	36.14	0.34	0.50	0.46	0.50	0.01	100.19	0.63	0.36	0.01
A30	72.49	72.34	72.74	0.25	25.75	25.57	25.93	0.18	0.45	0.42	0.46	0.02	98.69	0.73	0.26	0.01
								$Pd_{17}Se_{15}$								
A13	7.07	6.55	6.86	0.16	55.31	54.72	55.80	0.45	36.14	35.90	36.48	0.25	98.52	2.01	15.95	14.04
A15	6.10	5.93	6.23	0.15	56.29	56.20	56.72	0.26	36.56	36.46	37.40	0.47	98.95	1.73	16.15	14.13
A17	5.15	4.84	5.46	0.22	56.26	56.00	56.80	0.30	37.06	36.91	37.18	0.09	98.47	1.46	16.18	14.36
A18	6.88	6.82	6.94	0.06	54.05	53.59	54.51	0.46	38.48	38.30	38.65	0.18	99.41	1.93	15.35	14.72
A22	5.70	5.51	5.80	0.13	57.35	57.30	57.39	0.04	36.44	36.35	36.58	0.10	99.49	1.60	16.38	14.02
A23	5.11	4.68	5.45	0.32	57.34	57.14	57.55	0.17	37.03	36.81	37.30	0.20	99.49	1.44	16.34	14.22
A24	6.41	5.93	6.88	0.48	55.96	55.69	56.23	0.27	36.56	36.47	36.64	0.09	98.92	1.81	16.05	14.13
A25	4.94	4.68	5.20	0.26	57.45	57.34	57.55	0.10	37.14	36.98	37.30	0.16	99.53	1.39	16.36	14.25
A29	2.52	2.38	2.79	0.19	58.51	58.26	58.96	0.32	38.00	37.92	38.07	0.06	99.04	0.71	16.69	14.61
A31	4.54	4.40	4.68	0.14	57.99	57.81	58.17	0.18	36.34	36.10	36.59	0.25	98.87	1.31	16.73	13.97
A35	6.16	6.02	6.34	0.13	56.31	55.84	56.60	0.33	37.17	36.50	37.58	0.48	99.64	1.73	16.02	14.25
A36	7.01	6.16	6.85	0.16	56.17	56.54	55.79	0.38	37.00	36.97	37.03	0.03	100.17	1.99	15.98	14.19

d.l.: below detection limit
* experimental product at 430 °C

TABLE 4. – continued

wt.%	Ag				Pd				Se					*apfu*		
No.		Min	Max	Std.dev.		Min	Max	Std.dev.		Min	Max	Std.dev.	Total	Ag	Pd	Se
								$Pd_{34}Se_{11}$								
A23	d.l.				80.71	80.58	80.85	0.14	19.06	19.01	19.12	0.05	99.78		34.14	10.86
A25	0.29	0.22	0.38	0.07	81.34	81.27	81.46	0.09	18.78	18.76	18.79	0.01	100.41	0.12	34.23	10.65
								Pd_4Se								
A26	d.l.				84.61	83.88	85.67	0.55	15.29	15.02	15.40	0.13	99.91		4.02	0.98
A34	d.l.				84.65	84.32	85.15	0.31	15.33	15.15	15.51	0.12	99.98		4.02	0.98
								Pd_7Se_2								
A28	0.12	0.06	0.18	0.06	82.41	82.03	82.79	0.38	16.97	16.96	16.98	0.01	99.50	0.01	7.04	1.95
								Pd_7Se_4								
A31	d.l.				69.90	69.44	70.98	0.47	29.45	29.19	29.77	0.10	99.71		7.03	3.97
								$PdSe_2$								
A12	d.l.				40.21	39.96	40.48	0.21	57.95	57.96	58.18	0.19	98.18		1.02	1.98
A16	d.l.				40.92	40.33	41.63	0.54	58.18	57.89	58.64	0.33	99.17		1.03	1.97
A29	d.l.				41.21	40.78	41.63	0.43	58.27	57.89	58.64	0.38	99.57		1.02	1.98
								PdSe								
A33	d.l.				57.70	57.19	58.13	0.36	41.85	41.65	42.15	0.19	99.55		1.01	0.99
								Pd_9Se_2								
A3*	d.l.				85.10	58.04	85.17	0.07	14.07	13.99	14.14	0.08	99.17		9.00	2.00

d.l.: below detection limit

TABLE 5. STABLE ASSEMBLAGES IN THE SYSTEM Ag–Pd–Se at 350°C, 430°C, and 530°C

Stable assemblages in the Ag-Pd-Se system		
at 350 °C	at 430 °C	at 530 °C
Se_l + $PdSe_2$ + Ag_2Se	Se_l + $PdSe_2$ + Ag_2Se	Se_l + $PdSe_2$ + Ag_2Se
Ag_2Se + $PdSe_2$ + $Ag_2Pd_3Se_4$	Ag_2Se + $PdSe_2$ + $Pd_{17}Se_{15\ ss}$	Ag_2Se + $PdSe_2$ + $Pd_{17}Se_{15\ ss}$
PdSe + $PdSe_2$ + $Pd_{17}Se_{15\ ss}$	PdSe + $PdSe_2$ + $Pd_{17}Se_{15\ ss}$	PdSe + $PdSe_2$ + $Pd_{17}Se_{15\ ss}$
$Ag_2Pd_3Se_4$ + $PdSe_2$ + $Pd_{17}Se_{15\ ss}$	$(Ag,Pd)_{22}Se_{6\ ss}$ + $Pd_{17}Se_{15\ ss}$ + $AgPd_3Se_{\ ss}$	$(Ag,Pd)_{22}Se_{6\ ss}$ + $Pd_{17}Se_{15\ ss}$ + L_2
Ag_2Se + $Ag_2Pd_3Se_4$ + $Pd_{17}Se_{15\ ss}$	Ag_2Se + $(Ag,Pd)_{22}Se_{6\ ss}$ + $Pd_{17}Se_{15\ ss}$	$(Ag,Pd)_{22}Se_{6\ ss}$ + $AgPd_3Se_{\ ss}$ + L_2
Ag_2Se + $(Ag,Pd)_{22}Se_{6\ ss}$+ $Pd_{17}Se_{15\ ss}$	$AgPd_3Se_{\ ss}$ + $Pd_{17}Se_{15\ ss}$ + L_1	$Pd_{17}Se_{15\ ss}$ + $AgPd_3Se_{\ ss}$ + L_2
$Pd_{17}Se_{15\ ss}$ + Pd_7Se_4 + $Pd_{34}Se_{11}$	$AgPd_3Se_{\ ss}$ + Pd_7Se_2 + L_1	Ag_2Se + $(Ag,Pd)_{22}Se_{6\ ss}$+ $Pd_{17}Se_{15\ ss}$
$(Ag,Pd)_{22}Se_{6\ ss}$ + $Pd_{17}Se_{15\ ss}$ + $AgPd_3Se_{\ ss}$	$AgPd_3Se_{\ ss}$ + Pd_7Se_2 + $Ag_6Pd_{74}Se_{20}$	$AgPd_3Se_{\ ss}$ + $Pd_{17}Se_{15\ ss}$ + L_1
$AgPd_3Se_{\ ss}$ + $Pd_{17}Se_{15\ ss}$ + $Pd_{34}Se_{11}$	$Ag_6Pd_{74}Se_{20}$ + Pd_4Se + Pd_7Se_2	$AgPd_3Se_{\ ss}$ + Pd_7Se_2 + L_1
$AgPd_3Se_{\ ss}$ + $Pd_{34}Se_{11}$ + Pd_7Se_2	$Ag_6Pd_{74}Se_{20}$ + Pd_4Se + $Pd_9Se_{2\ ss}$	$AgPd_3Se_{\ ss}$ + Pd_7Se_2 + $Ag_6Pd_{74}Se_{20}$
$AgPd_3Se_{\ ss}$ + Pd_7Se_2 + Pd_4Se	$Ag_6Pd_{74}Se_{20}$ + $Pd_9Se_{2\ ss}$ + (Ag,Pd) alloy	$Ag_6Pd_{74}Se_{20}$ + Pd_4Se + Pd_7Se_2
$AgPd_3Se_{\ ss}$ + Pd_4Se + (Ag,Pd) alloy	$AgPd_3Se_{\ ss}$ + (Ag,Pd) alloy + $Ag_6Pd_{74}Se_{20}$	$Ag_6Pd_{74}Se_{20}$ + Pd_4Se + $Pd_9Se_{2\ ss}$
$AgPd_3Se_{\ ss}$ + $(Ag,Pd)_{22}Se_{6\ ss}$ + (Ag,Pd) alloy	$AgPd_3Se_{\ ss}$ + $(Ag,Pd)_{22}Se_{6\ ss}$ + (Ag,Pd) alloy	$Ag_6Pd_{74}Se_{20}$ + $Pd_9Se_{2\ ss}$ + (Ag,Pd) alloy
Ag_2Se + $(Ag,Pd)_{22}Se_{6\ ss}$ + (Ag,Pd) alloy	Ag_2Se + $(Ag,Pd)_{22}Se_{6\ ss}$ + (Ag,Pd) alloy	$AgPd_3Se_{\ ss}$ + $Ag_6Pd_{74}Se_{20}$ + (Ag,Pd) alloy
		$AgPd_3Se_{\ ss}$ + $(Ag,Pd)_{22}Se_{6\ ss}$ + (Ag,Pd) alloy
		Ag_2Se + $(Ag,Pd)_{22}Se_{6\ ss}$ + (Ag,Pd) alloy

The subscript "ss" indicates a solid solution.

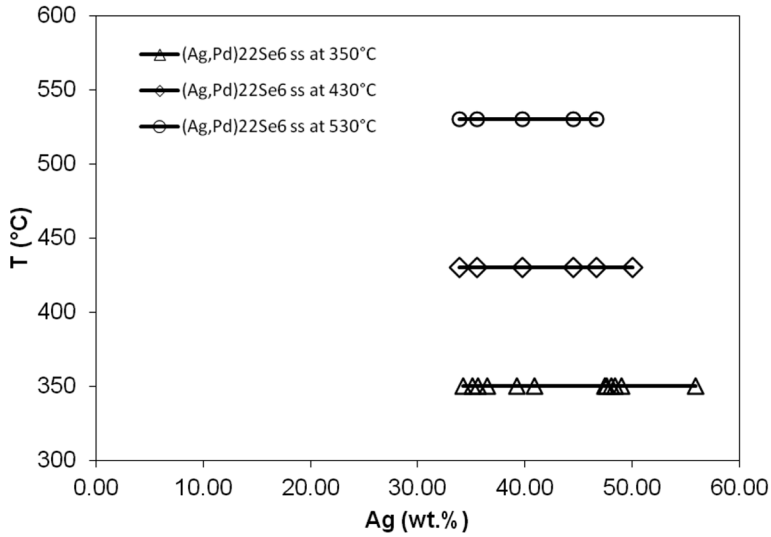

FIG. 4. Solubility of Ag in a $(Ag,Pd)_{22}Se_6$ solid solution with increasing temperature.

Phase relations at 530 °C

The isothermal section for 530 °C is shown in Figure 3c. At this temperature three ternary phases, $(Ag,Pd)_{22}Se_6$, $AgPd_3Se$, and $Ag_6Pd_{74}Se_{20}$, are stable in the system. The ternary eutectic liquid appears in the system between $(Ag_{11\pm x}Pd_{11\pm x})_{\Sigma 22}Se_{6ss}$, $Ag_{1-x}Pd_{3+x}Se_{ss}$, and $Pd_{17}Se_{15\ ss}$. Subsequently, assemblages L_2 + $Ag_{11\pm x}Pd_{11\pm x}Se_{6\ ss}$ + $Pd_{17}Se_{15\ ss;}$ L_2 + $Ag_{11\pm x}Pd_{11\pm x}Se_{6\ ss}$ + $Ag_{1-x}Pd_{3+x}Se_{\ ss}$; and L_2 + $Pd_{17}Se_{15\ ss}$ + $Ag_{1-x}Pd_{3+x}Se_{\ ss}$ become stable (Table 5). The solid solution $(Ag_{11\pm x}Pd_{11\pm x})_{\Sigma 22}Se_6$ extends from $(Ag_{8.99}Pd_{13.11})_{\Sigma 22.11}Se_{5.89}$ (33.9 wt.% Ag) to $(Ag_{13.29}Pd_{8.93})_{\Sigma 22.22}Se_{5.78}$ (44.6 wt.% Ag) at 530 °C.

Minerals and Phases, Potential New Minerals

Binary phases

Palladseite. The experimental results show that the synthetic analogue of the mineral palladseite, $Pd_{17}Se_{15}$, forms a limited solid solution and dissolves up to 7 wt.% Ag. Silver substitutes for Pd and also for Se in the structure of $Pd_{17}Se_{15}$. In nature palladseite always contains some Cu (up to 4 wt.%), Hg (up to 3 wt.%; Davis *et al*. 1977, Olivo & Gauthier 1995), and also Pt (up to 3.5 wt.%), Ag, and Fe (Cabral *et al*. 2002, Cabral & Lehmann 2007). According to data available for natural palladseite, these elements substitute for both Pd and Se. Palladseite is stable up to 680 °C (Olsen *et al*. 1979). Palladseite was described from Itabira as an unnamed mineral by Clark *et al*. (1974), and was later identified as palladseite by Davis *et al*. (1977); it was also subsequently observed by Olivo & Gauthier (1995), Cabral *et al*. (2002), and Cabral & Lehmann (2007). In the Cauê iron mine in Itabira palladseite, palladian gold, and arsenopalladinite were formed during the main hypogene ore-forming event, where Pd (and Au) was likely transported as chlorine complexes by oxidized saline brines, and palladseite deposited as a result of changes in pH or oxygen fugacity (Olivo & Gammons 1996).

Verbeekite. According to the XRD powder data, the synthetic phase $PdSe_2$ at the studied temperature interval 350–550 °C is orthorhombic (Table 1; Grønvold & Røst 1957, Vymazalová *et al*. 2011). Its natural monoclinic analogue (Table 2), the mineral verbeekite (Roberts *et al*. 2002), could not be synthesized. Even long term (nine months) heating at 100 °C was not successful in obtaining the monoclinic variety of the $PdSe_2$ phase. The mineral verbeekite is rather rare; it was reported from the Musonoi deposit (Roberts *et al*. 2002) and Hope's Nose (Paar *et al*. 1998); in both localities it is considered to be a primary phase. At Hope's Nose, fluid inclusion studies (Stanley *et al*. 1990) suggest that selenide minerals formed from hydrothermal solutions at low temperatures in a range from 65 to 120 °C. This supports the experimental study and the formation of veerbekite below 100 °C.

Naumannite. The phase Ag_2Se was observed only in its low temperature orthorhombic modification, an analogue of the mineral naumannite, in all experiments. It was not possible to obtain the cubic beta modification of the phase Ag_2Se experimentally, as the process of rapid quenching causes the phase to transform to its orthorhombic, low-temperature alpha modification (Billetter & Ruschewitz 2008).

Under natural conditions the presence of naumannite defines the minimum Se fugacity conditions required to form selenide-bearing deposits (Simon *at al*. 1997). Naumanite is one of the dominant selenide minerals in Au-Ag epithermal deposits. Those types of deposits characteristically have a low fugacity Se/S ratio that prevents formation of other selenides, thus allowing significant amounts of Se to substitute for S in sulfides (Simon *et al*. 1997).

Pd_9Se_2. The Pd_9Se_2 phase is stable in temperature range 390 to 635 °C (Takabatake *et al*. 1987). A natural occurrence of Pd_9Se_2 was reported from the Serra Pelada Au-Pd-Pt deposit, northern Brazil by Cabral *et al*. (2002) and Cabral & Lehmann (2007). The thermal stability of the phase is not in agreement with the temperature of formation of the Serra Pelada mineralization (below 150 °C) (Cabral & Lehmann 2007). The phase Pd_9Se_2 is probably stabilized by another element (Pt or Au) at lower temperature in nature, or it corresponds to other palladium selenides (likely the phase Pd_4Se), but an X-ray study of the natural phase is desirable.

Ternary phases

In the Ag–Pd–Se system four ternary compounds were detected: the phase $Ag_2Pd_3Se_4$, analogue of the mineral chrisstanleyite, and the phases $AgPd_3Se$, $(Ag,Pd)_{22}Se_6$, and $Ag_6Pd_{74}Se_{20}$.

Chrisstanleyite. The powder XRD data for $Ag_2Pd_3Se_4$ at 350 ºC are in agreement with the crystal structure data determined by Topa *et al*. (2006) for natural $Ag_2Pd_3Se_4$, the mineral chrisstanleyite. The unit cell parameters for synthetic chrisstanleyite are given in Table 1. The phase is stable up to 430 ºC. The phase $Ag_2Pd_3Se_4$ forms stable association with naumannite (Ag_2Se) and veerbekite ($PdSe_2$) (Fig. 5a). It also coexists with palladseite (dissolving 7 wt.% Ag) (Fig. 3a). In nature chrisstanleyite occurs with veerbekite (from Musonoi, Roberts *et al*. 2002; Hope's Nose, Paar *et al*. 1998) and other palladium selenides, such as milotaite (from Předbořice, Paar *et al*. 2005), jaguéite (from El Chire, Paar *et al*. 2004), tichendorfite (from Harz Mountains, Stanley *et al*. 2002, and Gongo Soco, Cabral & Lehmann 2007), or oosterboschite (Copper Hills in the East Pilbara region, Nickel 2002 and Musonoi, Roberts *et al*. 2002), among other selenides, native gold, and silver.

$AgPd_3Se$. This phase has a compositional range from Ag 18.3 wt.% to Ag 21.6 wt% (Table 4). The crystal structure of the phase was determined by Laufek *et al*. (2011; Table 1). The $AgPd_3Se$ phase is cubic; the solid solution $Ag_{1-x}Pd_{3+x}Se$ extends to $x = 0.15$, while the unit cell parameter changes from a 8.632(1) Å (at $x = 0$; 18.3 wt.% Ag, experiment A28) to 8.6155(6) Å (at $x = 0.15$; 21,4 wt.% Ag, experiment A21). The unit cell parameters increase with higher Ag contents. The range of solid solution is consistent in the studied temperate range (350–530 ºC; Fig 3.a, b, c). The strongest five lines of the X-ray diffraction pattern [d in Å (I) (hkl)] are: 2.3925(85)(302)**,** 2.3057(100)(231,321)**,** 2.1569(51)(004), 2.0925(46)(410,322), 1.8829(49)(241,421).

The $AgPd_3Se$ phase coexists with $(Ag,Pd)_{22}Se_6$ and palladseite, Fig 5b. The phase also forms stable associations with palladium binary selenides (Fig. 3a) unidentified in nature to date. In such mineral assemblages the phase $AgPd_3Se$ can be expected to be found in nature, particularly in the presence of palladseite and its conditions of formation, like auriferous mineralization in Minas Gerais and Serra Pelada in Brazil.

$(Ag,Pd)_{22}Se_6$. The ternary $(Ag,Pd)_{22}Se_6$ phase forms a broad solid solution $(Ag_{11\pm x}Pd_{11\pm x})_{22}Se_6$ where $0.2 \geq x \geq 3.9$. Silver substitutes for Pd in the $(Ag_{11\pm x}Pd_{11\pm x})_{22}Se_6$ structure with an almost constant Se content (Table 2). The solubility of Ag decreases with increasing temperature (Fig. 4). The $(Ag,Pd)_{22}Se_6$ phase is cubic; the crystal structure was determined by Laufek *et al*. (2013). The strongest five lines of the X-ray diffraction pattern [*d* in Å (I) (*hkl*)] are: 2.8267(28)(331), 2.3704(100)(511,333), 2.0524(73)(600,442), 1.8779(23)(335), 1.4513(55) (660,822). The unit cell parameters linearly increase with the Ag content from *a* 12.2697(5) Å (34 wt.% Ag, experiment A22) to 12.4143(9) Å (56 wt.% Ag, experiment A20).

$(Ag,Pd)_{22}Se_6$ forms stable associations with palladseite and $AgPd_3Se$ (Fig. 5b). In nature it can also be expected in mineral assemblages with the mineral palladseite. It also coexists with naumannite.

$Ag_6Pd_{74}Se_{20}$. This ternary phase appears in the system at 430 ºC. Its crystal structure is unknown and requires further investigation. Our evaluation of the X-ray powder-diffraction data, in terms of crystal structure determination and peak indexing, was not successful. Auto-indexing did not succeed. Some difficulties in X-ray data evaluation of the phase $Ag_6Pd_{74}Se_{20}$ may have been caused by the presence of Pd_9Se_2 in the sample. The strongest five lines of the X-ray diffraction pattern [*d* in Å(I)] are: 2.3318(68), 2.2935(91), 2.2845(100), 2.2587(61) 2.1004(64).

The phase forms stable associations with $AgPd_3Se$ and Pd_7Se_2. It also coexists with phases Pd_4Se and Pd_9Se_2. In nature the phase can be expected in a less traditional environment than is known for selenides, at temperatures of formation above 430 ºC, likely in association with the phase Pd_9Se_2.

Conclusions and Implications

1. The phase relations in the system Ag–Pd–Se have been studied at three isothermal sections at 350, 430, and 530 °C.

2. Four ternary phases were identified in the system: $Ag_2Pd_3Se_4$, the analogue of the mineral chrisstanleyite, and phases $AgPd_3Se$, $(Ag,Pd)_{22}Se_6$, and $Ag_7Pd_{73}Se_{20}$. The phase $Ag_2Pd_3Se_4$ is stable up to 430 ºC and at this temperature $Ag_7Pd_{73}Se_{20}$ appears in the system.

3. The phase $Pd_{17}Se_{15}$, the analogue of palladseite, dissolves up to 7 wt.% Ag, and the phase Pd_9Se_2 dissolves up to 3 wt.% Ag. The phase $AgPd_3Se$ forms a narrow solid solution $Ag_{1-x}Pd_{3+x}Se$ where *x* varies from 0 to 0.15. The range remains constant with increasing temperature. The phase $(Ag,Pd)_{22}Se_6$ forms an extensive solid solution $(Ag_{11\pm x}Pd_{11\pm x})_{22}Se_6$ with $0.2 \geq x \geq 3.9$, at 350 ºC. The solid solution decreases towards Ag with increasing temperature. Silver substitutes for Pd in the $AgPd_3Se$ and $(Ag,Pd)_{22}Se_6$ structures.

4. The phase $Ag_2Pd_3Se_4$, the analogue of the mineral chrisstanleyite, forms a stable association with naumannite (Ag_2Se) and veerbekite ($PdSe_2$); it also coexists with palladseite (dissolving 7 wt.% Ag). This phase is stable up to 430 ºC.

5. Phase relations determined the mineral assemblages that can be expected to occur in nature. Ternary phases $AgPd_3Se$ and $(Ag,Pd)_{22}Se_6$ and binary phases PdSe, Pd_7Se_4, and $Pd_{34}Se_{11}$ can be expected in associations with the mineral palladseite, among other selenides. Finding these phases is highly probable in telethermal selenide veins and unconformity-related uranium types of deposits, at conditions of high fugacity Se/S ratio, an oxidizing environment, and Se-rich

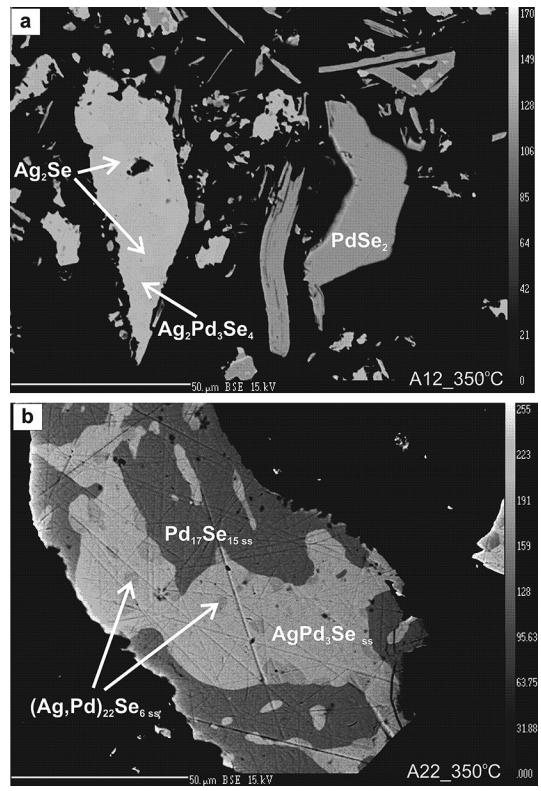

FIG. 5. BSE (backscattered electron) images illustrating the assemblages (a) chrisstanleyite ($Ag_2Pd_3Se_4$) + naumanite (Ag_2Se) + $PdSe_2$, (experiment A12, 350 °C), (b) $AgPd_3Se$ ss + palladseite ($Pd_{17}Se_{15}$) ss + $(Ag,Pd)_{22}Se_6$ ss (experiment A22, 350 °C).

fluids, forming at low temperatures. These phases can be expected particularly at mineralizations where other Pd selenides are already known to occur, such as Au-Pd mineralization in Itabira, Minais Gerais (Brazil), selenide mineralization in the Harz Mountains (Germany), Hope's Nose (England), La Rioja province (Argentina), or Musonoi (D.R. Congo). The appearance of Pd (-Ag) selenides can be also expected in black shale deposits like Kupferschiefer-type deposits or other metal-rich black shales.

6. The phase $Ag_6Pd_{74}Se_{20}$ forms stable associations with $AgPd_3Se$ and Pd_7Se_2. It also coexists with Pd_4Se and Pd_9Se_2. This phase is stable above 430 ºC. In nature, $Ag_6Pd_{74}Se_{20}$ and Pd_9Se_2 can be expected to occur in a less traditional environment than is known for selenides, forming at higher temperatures (above 430 ºC).

Acknowledgements

Financial support through grant no. P210/11/P744 from the Grant Agency of the Czech Republic; the project LA 11125 / KONTAKT II from the Ministry of Education, Youth and Sports of the Czech Republic; a grant of the President of the Russian Federation for State Support of Young Russian Scientists (MK-1557.2011.5); and grant no. 12-05-31418 from the Russian Foundation for Basic Research are gratefully acknowledged. The authors are grateful to Dr. Vlasta Böhmová (Institute of Geology AS CR) for carrying out the electron-microprobe analyses. Comments by Associate Editor Chris Ballhaus, Louis Cabri, and an anonymous referee are greatly appreciated; they helped to improve this paper. We also thank Lee A. Groat and Mackenzie Parker for their careful editing.

References

Ahlfeld, F. (1941) El yacimiento de selenio de Pacajake. *Ministerio de la Economia Nacional Boletin Informativo, La Paz, Bolivia* **1(2)**, 23–28.

Billetter, H. & Ruschewitz, U. (2008) Structural Phase Transitions in Ag_2Se (Naumanite). *Zeitschrift für Anorganische und Allgemeine Chemie* **634**, 241–246.

Cabral, A.R. & Lehmann, B. (2007) Seleniferous minerals of palladium and platinum from ouro preto-bearing mineralization in Brazil. *Ore Geology Reviews* **32**, 681–688.

Cabral, A.R., Lehmann, B., Kwitko, R., Galbiatti, H.F., & Pereira, M.C. (2002) Palladseite and its oxidation: evidence from Au-Pd vein-type mineralization (jacutinga), Cuaê iron-ore mine, Quadrilátero Ferrífero, Minas Gerais, Brazil. *Mineralogical Magazine* **66(2)**, 327–336.

Clark, A.M., Criddle, A.J., & Fejer, E.E. (1974) Palladium arsenide-antimonides from Itabira, Minas Gerais, Brazil. *Mineralogical Magazine* **39**, 528–543.

Davis, R.J., Clark, A.M., & Criddle, A.J. (1977) Palladseite, a new mineral from Itabira, Minas Gerais, Brazil. *Mineralogical Magazine*. **41(123)**, M10–M13.

Geller, S. (1962) The crystal structure of $Pd_{17}Se_{15}$. *Acta Crystallographica* **15**, 713–721.

Grønvold, F. & Røst, E. (1957) The crystal structure of $PdSe_2$ and PdS_2. *Acta Crystallographica* **10**, 329–331.

Grønvold, F. & Røst, E. (1962) The crystal structure of Pd_4Se and Pd_4S. *Acta Crystallographica* **15**, 11–13.

Grundmann, G., Lehrberger, G., & Schnorrer-Köhler, G. (1990) The El Dragón mine, Potosi, Bolivia. *Mineralogical Record **21**,* 133–146.

Hansen, M. & Anderko, K. (1958) *Constitution of binary alloys*. McGrow-Hill, New York, United States.

Ijjaali, I. & Ibers, J.A. (2001) Crysral structure of palladium selenide, PdSe. *Zeitschrift für Kristallographie* **216**, 485–486.

Johan, Z. (1989) Merenskyite, $Pd(Te,Se)_2$, and the low-temperature selenide association from the Předbořice uranium deposit, Czechoslovakia. *Neues Jahrbuch für Mineralogie (Monatshefte)* **4**, 179–191.

Johan, Z., Picot, P., & Ruhlmann, F. (1982) Evolution paragénétique de la mineralisation uranifere de Chameane (Puy-de-Dome), France: Chameanite, geffroyite et giraudite, trois seleniures nouveaux de Cu, Fe, Ag et As. *Tschermaks Mineralogische und Petrographische Mitteilungen* **29**, 151–165.

Karakaya, I. & Thompson W.T. (1988) The Ag-Pd (silver-palladium) system. *Bulletin of Alloy Phase Diagrams* **9(3)**, 237–243.

Karakaya, I. & Thompson, W.T. (1990) The Ag-Se (silver-selenium) system. *Bulletin of Alloy Phase Diagrams* **11(3)**, 266–271.

Kullerud, G. (1971) Experimental techniques in dry sulfide research. *In* Research Techniques for High Pressure and High Temperature (G.C. Ulmer, ed.). Spinger-Verlag, New York,United States, 288–315.

Kvaček, M. (1979) Selenides from the deposits of western Moravia, Czechoslovakia. *Acta Universitatis Carolinae-Geologica* **1(2)**, 15–38

Laufek, F., Vymazalová, A., Chareev, D.A., Kristavchuk, A.V., Lin, Q., Drahokoupil, J., & Vasilchikova, T.M. (2011) Crystal and electronic structure study of $AgPd_3Se$. *Journal of Solid State Chemistry* **184(10)**, 2794–2798.

Laufek, F., Vymazalová, A., Chareev, D., Kristavchuk, A., Drahokoupil, J., & Voronin, M.A. (2013) Synthesis and crystal structure of $(Ag,Pd)_{22}Se_6$ (PD-2012-0053). *Powder Diffraction* **28(1)**, 13–17.

MATKOVIC, T. & SCHUBERT, S. (1978) Kristallstruktur von Pd_7Se_4. *Journal of the Less-Common Metals* **59**, P57–P63.

NICKEL, E.H. (2002) An unusual occurence of Pd,Pt, Au, Ag and Hg minerals in the Pilbara Region of Western Australia. *Canadian Mineralogist* **40**, 419–433.

OKAMOTO, H. (1992) The Pd-Se (palladium - selenium) system. *Journal of Phase Equilibria* **13(1)**, 69–72.

OLIVO, G.R. & GAMMONS, C.H. (1996) Thermodynamic and textural evidence for at least two stages of A-Pd mineralization at the Cauê iron mine, Itabira district, Brazil. *Canadian Mineralogist* 34, 547–557.

OLIVO, G.R. & GAUTHIER, M. (1995) Palladium minerals from the Cauê iron mine, Itabira district, Minas Gerais, Brazil. *Mineralogical Magazine* **59**, 455–463.

OLSEN, T., RIST, E., & GRØNVOLD, F. (1979) Phase relations of palladium selenides. *Acta Chemica Scandinavica* **33(4)**, 251–256.

PAAR, W.H., SUREDA, R.J., & DE BRODTKORB, M.K. (1996) Oro y plata en los yacimientos de selenio de La Rioja, Argentina: hallazgo de fischesserita, Ag_3AuSe_2. III Reunion de Mineralogía y Metalogenia. *Publicación del Instituto de Recursos Minerales (Universidad Nacional de la Plata)* **5**, 177–185.

PAAR, W.H., ROBERTS, A.C., CRIDDLE, A.J., & TOPA, D. (1998) A new mineral, chrisstanleyite, $Ag_2Pd_3Se_4$, from Hope`s Nose, Torquay, Devon, England. *Mineralogical Magazine* **6,** 257–264.

PAAR, W.H., TOPA, D., MAKOVICKY, E., & CULETTO, F.J. (2005) Milotaite, PdSbSe, a new palladium mineral species from Předbořice, Czech Republic. *Canadian Mineralogist* **43**, 689–694.

PAAR, W.H., TOPA, D., MAKOVICKY, E., SUREDA, R.J., DE BRODTKORB, M.K., NICKEL E.H., & PUTZ, H. (2004) Jaqueite, $Cu_2Pd_3Se_4$, a new mineral species from El Chire, La Rioja, Argentina. *Canadian Mineralogist* 42, 1745–1755.

RAHLFS, P. (1936) Uber die kubischen Hochtemperatur modifikationen der Sulfide, Selenide und Telluride des Silbers und des einwertigen Kupfers. Zeitschrift für Physikalische Chemie B37, 157–194.

ROBERTS, A.C., PAAR, W.H., COOPER, M.A., TOPA, D., CRIDDLE, A.J., & JEDWAB, J. (2002) Verbeekite, monoclinic $PdSe_2$, a new mineral from the Musonoi Cu-Co-Mn-U mine, near Kolwezi, Shaba Province, Democratic Republic of Congo. *Mineralogial Magazine* **66(1)**, 173–179.

ROBINSON, S.C. (1955) Mineralogy of uranium deposits, Goldfields, Saskatchewan. *Geological Survey of Canada Bulletin* **31**, 128p.

RODRÍGUEZ-CARVAJAL, J. (2006) FullProf.2k: Rietveld Profile Matching & Integrated Intensities Refinement of X-ray and/or Neutron Data (powder and/or single-crystal). Laboratoire Léon Brillouin, Centre d´Etudes de Saclay, Gif-sur-Yvette Cedex, France.

RUDASHEVSKIY, N.S., KNAUF, V.V., & CHERNYSHOV, N.M. (1995) Platinum-group minerals from Kurs magnetic anomaly black shales. *Doklady Akademii Nauk* **344(1)**, 91–95.

SATO, S., TAKABATAKE, T., & ISHIKAWA, M. (1989) Structures of superconducting palladium selenides, Pd_7Se_2 and $Pd_{34}Se_{11}$. *Acta Crystallographica* **C45**, 1–3.

SIMON, G. & ESSENE, E.J. (1996) Phase relations among selenides, tellurides, and oxides. I. Thermodynamic properties and calculated equilibria. *Economic Geology* **92**, 468–484.

SIMON, G., KESLER, S.E., & ESSENE E.J. (1997) Phase relations among selenides, sulphides, tellurides, and oxides: II.Applications to selenide-bearing ore deposits. *Economic Geology* **92**, 468–484.

STANLEY, C.J., CRIDDLE, A.J., & LLOYD, D. (1990) Precious and base metal selenide mineralization at Hopes Nose, Torquay, Devon. *Mineralogical Magazine* **54**, 485–493.

STANLEY, C.J., CRIDDLE, A.J., FÖRSTER, H.-J., & ROBERTS, A.C. (2002) Tischendorfite, $Pd_8Hg_3Se_9$, a new mineral species from Tilkerode, Harz Mountains, Germany. *Canadian Mineralogist* **40**, 739–725.

TAKABATAKE, T., ISHIKAWA, M., & JORDA, J.L. (1987) Superconductivity and phase relations in the Pd-Se system. *Journal of the Less-Common Metals* **134**, 79–89.

TISCHENDORF, G. (1959) Zur Genesis einiger Selenid-vorkommen, insbesondere von Tilkerode im Harz. *Freiburg Forschungshefte Hamburg* **C208**.

TOPA, D., MAKOVICKY, E., & BALIC-ŽUNIC, T. (2006) The crystal structure of jagueite, $Cu_2Pd_3Se_4$, and chrisstanleyite, $Ag_2Pd_3Se_4$. *Canadian Mineralogist* **44**, 497–505.

VYMAZALOVÁ, A., DRÁBEK, M., & LAUFEK, F. (2011) Mineralogical significance of the system Pd-Se at 350°C. *In* Let`s talk ore deposits (E.Campos, ed.). Proceedings of the 11th Biennial SGA Meeting, Antofagasta, Chile. 660–662.

WALLIS, E. (1994) *Erzparagenetische und mineralchemische Untersuchung der Selenide in Harz*. Unpublished Diploma thesis, University of Hamburg, Hamburg, Germany.

WIEGERS, G.A. (1971) The crystal structure of the low-temperature form of silver selenide. *American Mineralogist* **56**, 1882–1888.

Received March 27, 2013, revised manuscript accepted February 24, 2014.